Broadband CSEM-guided starting model for full waveform inversion – Impact in the Brazilian deep offshore

Andrea Zerilli*, Fabio Miotti, Marco Mantovani, Schlumberger, Paulo T. L. Menezes, João L. Silva Crepaldi, Petrobras E&P/GEOF/MNS

Abstract

We present the potential of broadband marine Controlled Source Electromagnetics (CSEM) coupled with a Resistivity-to-Velocity transform workflow as a cost-effective starting model building for Full Waveform Inversion (FWI) to improve complex subsalt and around salt imaging.
The key aspect is the Resistivity-to-Velocity transform that provides more accurate and reliable velocity fields than those computed from tomography therefore alleviating FWI associated non-uniqueness and nonlinearity.
A case study is presented from an ultra-deep water area of the Espirito Santo Basin, offshore Brazil, where the presence of complex allochthonous salt makes around-salt and subsalt seismic depth imaging extremely challenging. The FWI final velocity model clearly shows that the broadband CSEM – Resistivity-to-Velocity model confirms to be an accurate and reliable starting model, successfully producing the correct updating direction.

Introduction

High-quality imaging of seismic data from complex geology requires an accurate model of the subsurface velocity field. In real life this may not be achievable. A velocity model is usually obtained using a depth tomography method on seismic data. However building models of complex salt bodies is often related to finding the correct shape of the bodies after sufficiently accurate background velocities are constructed. [i.e. Jones and Davison, 2014].
While most of the progress has come through new seismic acquisition technologies, such as wide-azimuth (WAZ), full-azimuth (FAZ), imaging through the incorporation of better physics has come in the form of FWI and Reverse Time Migration (RTM) producing the final 'images'.
Although the improvements have been very significant the associated time/cost factor relative to survey size and objectives might become prohibitive and illumination can still be poor caused by very complex salt.
Additional geophysical measurements such as deep-reading EM and potential fields [i.e. De Stefano et al., 2011; Moorkamp et al., 2011; Medina et al.; 2012; Panzner et al., 2014] are proving to provide key complementary information to constrain and define complex salt geometries and velocity distribution and thus improve depth imaging through velocity model building integrated workflows.
Recently [Zerilli et al., 2013, 2016] have revealed the potential of a new Integrated Ocean Bottom Geophysics (OBG) 'hybrid' Simultaneous Joint Inversion (SJI**)** and of a new Resistivity-to-Velocity transform workflow addressing the critical steps in around-salt and subsalt imaging and have shown that these workflows achieve seismic – EM integration for enhanced velocity model building and superior depth imaging through RTM in complex salt such as ones encountered in the Espirito Santo Basin.
Here we show that these enhanced models ensure cost-effective sufficiently accurate and reliable starting models for FWI.

Espirito Santo Ocean Bottom Geophysics data

The Espirito Santo research OBG acquisition (Figure 1) was carried out with the objective of obtaining multi-offset, multi-component, broadband CSEM and Magnetotelluric (MT) data that could support the interval velocity-depth model building in areas of low seismic sensitivity such as the around-salt, intra-salt and subsalt sections of the basin. A total of 434 km of CSEM towlines were towed twice over the same 157 static point receivers. The base frequency was 0.25 Hz for towlines 01Tx001, 02Tx001, 03Tx001 and 0.0625 Hz for towlines 01Tx002, 02Tx002, 03Tx002. Five harmonics (0.75, 1.25, 2.25, 2.75, 3.25 Hz) were computed from the 0.25 Hz base frequency and four (0.1875, 0.3125, 0.5625, 0.8125 Hz) from the 0.0625 Hz.
The increased number of frequencies determined from previous sensitivity analysis made the data richer in potential bandwidth and resolution for enhanced complex overburden, 'deep' subsalt and around-salt imaging. The recorded data were of very good quality and achieved interpretable offsets exceeding 25 km for the lowest frequencies. An extended deployment period allowed for the acquisition of collocated MT data.
The resistivity distribution recovered by a 3D 'mesh'-based inversion was used as a 'background' model for a 'structure'- based inversion introducing boundary-preserving constraints to preserve sharp contrast at the 'allochtonous' BOS boundaries and give better estimation of salt resistivities. Figure 2 shows the 3D inversion results along the L_QQ slice (middle line in Figure 1). The allochtonous salt body B_{QQ} steeply dipping flank walls and an Early Tertiary minibasin are imaged with increased resolution thus reducing the ambiguity in interpretation and for the prospectivity of the basin. Most importantly, Figure 2 clearly shows that BOS was determined to be

about 300 to 700 meters shallower than that interpreted from NAZ only-seismic.

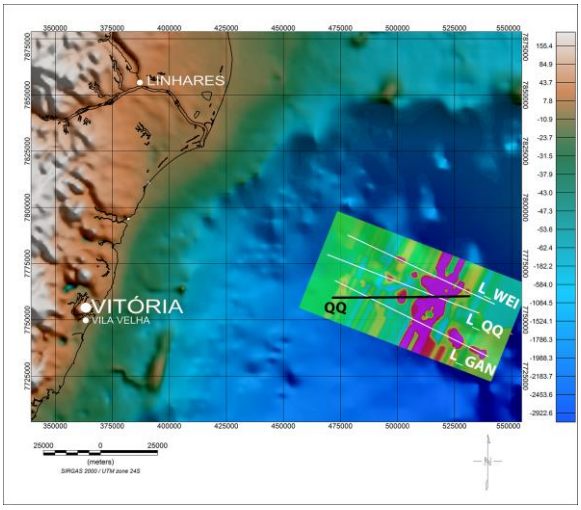

Figure 1. Espirito Santo demonstration research Ocean Bottom Geophysics survey location with vertical resistivity depth slice from 3D CSEM inversion extracted at -3500 meters b.m.s.l.

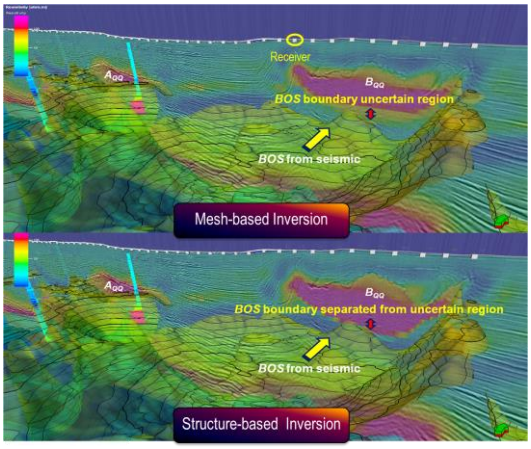

Figure 2. Vertical resistivity from 3D 'mesh'-based (upper panel) and 'structure'-based (lower panel) inversions along L_QQ. BOS, width and magnitude at the center of the 'allochthonous' salt bodies accurately imaged. Green surface with contours corresponds to BOS from NAZ only-seismic interpretation.

Multi-physics velocity model building workflows

[Zerilli et al., 2013] have presented the SJI inversion results of modeled ultra-long offset first arrival traveltime seismic and EM static point receiver data to prove the strength and efficiency of SJI to retrieve complex around-salt, subsalt velocity models without resorting to as full an azimuth as possible towed-streamer acquisition and high-time, computer intensive depth migration.

In the absence of collocated ultra-long offset OB seismic, the Resistivity-to-Velocity transform workflow was introduced [Zerilli et al., 2016] to derive velocity models from resistivity models computed from broadband CSEM inversion therefore taking advantages of the greater resolving power of EM to map high resistive structures (such as salt) embedded in conductive sedimentary sequences.

The Resistivity-to-Velocity transform workflow was developed applying the Hacikoylu's petrophysical cross-property relation and uncertainty analysis of the data and the model [Hacikoylu et al., 2006; Zerilli et al., 2016].

This workflow applied to the Espirito Santo data consisted of two phases:

1. Calibration of the Hacikoylu's law at well log scale to determine the law's coefficients.

2. Application of the calibrated Hacikoylu's law on the model(s) derived from the 3D EM inversions to obtain the P-Velocity distribution. This includes the model down-scaling required to interpolate the coefficients from the wells into the 3D-model mesh.

The Hacikoylu's coefficients were estimated using the following derived-log measurements: cumulative slowness, η_c (s/m), cumulative velocity, V_p (km/s), cumulative conductance σ_c (S/m), transverse resistance T_R ($\Omega \cdot m^2$), conductance σ (S/m) and compressional slowness η (s/m).

Figure 3 shows the velocity model along the 'QQ' line (black line in Figure 1) from NAZ only-seismic depth tomography, while Figure 4 shows the result of the 3D EM inversion along the same section. The result of the Resistivity-to-Velocity transform along the same line is shown in Figure 5.

The comparison between the velocity models of Figure 3 and Figure 5 highlights the features added by the Resistivity-to-Velocity transform. The results show that large resistivity contrasts around salt and the ability of EM to map supra-salt, steep dipping salt complex geometries and resistivity contrasts directly below BOS, translate into a transformed velocity model with more complex salt overburden and lower velocities just below BOS that may indicate the spatial distribution of salt exit velocities.

The transformed velocity model retrieving the long and middle-wavelength components and showing significant improvements of supra-salt, ToS, flanks, BOS and salt exit geometries provides more accurate and reliable features than those computed from tomography, therefore making RTM migration less sensitive to model errors leading to the reduction or collapse of the imaging cycle [Zerilli et al., 2016].

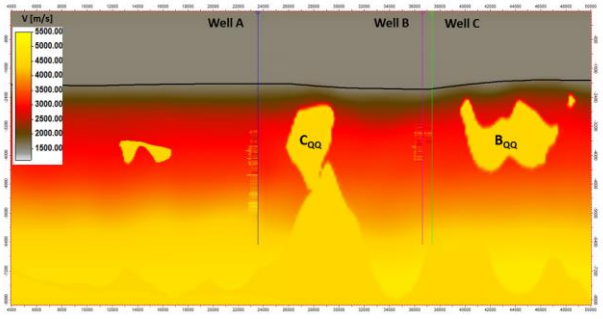

Figure 3. Line QQ – P-Velocity interpreted from NAZ only-seismic. Tie with velocity logs provided by the area wells.

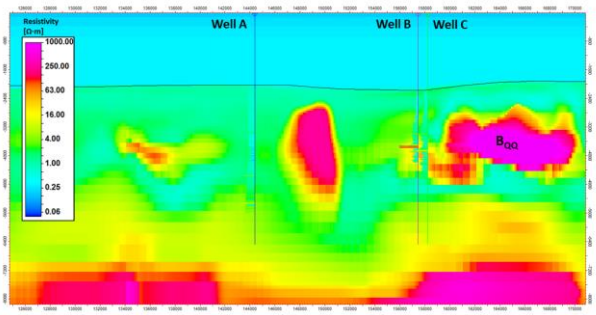

Figure 4 Line QQ – Vertical resistivity from 3D 'structure'-based inversion of the broadband CSEM data. Tie with resistivity logs provided by the area wells.

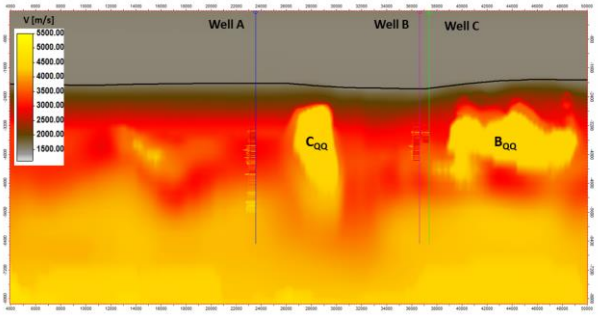

Figure 5 Line QQ – P-Velocity from the broadband CSEM – Resistivity-to-Velocity transform workflow. Tie with velocity logs provided by the area wells.

Ensuring starting model adequacy for FWI

Building sufficiently accurate starting model remains one of the most topical issue for successful application of FWI. The approach we are proposing here relies on the broadband CSEM – Resistivity-to-Velocity transform workflow as a cost- effective alternative to link and exploit the complementary information that EM data may provide to define and constrain complex salt geometries and salt, around-salt, subsalt velocity distribution and mitigate the drawbacks of model building based on seismic only.

The broadband CSEM – Resistivity-to-Velocity model contains the vertical wavenumbers that are missing from an 'inadequate-acquisition' seismic low frequency and contributes to fill the spectral gap between model and seismic minimum frequency. The accuracy and reliability of the model is considered high at the chosen frequency for FWI, being built from inversion of low frequency EM data. The broadband CSEM – Resistivity-to-Velocity model reliability was checked versus its Kirchhoff Pre-Stack Depth Migration response and analysis of its residuals, showing surprisingly improved seismic image gathers [Zerilli et al., 2016].

The broadband CSEM – Resistivity-to-Velocity model contains the velocities but not the relevant fields for anisotropy, therefore isotropic FWI was run.

The inversion statistics indicate that the objective function is satisfactorily reduced by the prediction generated by the broadband CSEM – Resistivity-to-Velocity used as a starting model.

A set of selected gathers comparing modelled and observed data were used as FWI Quality Control (Figure 6). Predicted and observed gathers are both displayed in the FWI inversion bandwidth. The FWI final model is able to predict the relevant data features at this frequency. No evidence of cycle skips is detected in the QC.

The RTM stack responses of the final FWI model (Figures 7-8) show significant imaging improvement in the delineation of salt geometries, with particular reference to ToS. In the supra-salt sedimentary sequence, FWI is capable of uplifting the overall solution, re-iterating that the 'shallow' overburden is still poorly illuminated by the broadband CSEM data used in the Resistivity-to-Velocity workflow requiring additional higher frequencies, therefore not well constrained in the FWI starting model.

The FWI final velocity model clearly shows a better geological match with the corresponding RTM image on small scale features (Figures 9-10). It's worth noting that neither sonic nor check-shot well velocities were used to validate the data.

The FWI final model also shows that the broadband CSEM – Resistivity-to-Velocity model confirms to be an accurate and reliable starting model, successfully producing the correct updating direction although, lack of anisotropic characterization, as well as insufficient azimuth in the available seismic data, might have biased its full application potential.

Conclusion

In this work we have proposed to use a broadband CSEM – Resistivity-to-Velocity transformed model as a cost-effective starting model for FWI to improve complex subsalt and around salt imaging. The novel aspect is the Resistivity-to-Velocity transform that may provide more accurate and reliable velocity models than those computed from tomography therefore alleviating FWI associated non-uniqueness and nonlinearity.

The Espirito Santo FWI final velocity model clearly shows that the broadband CSEM – Resistivity-to-Velocity model confirmed to be an accurate and reliable starting model for FWI, successfully producing the correct updating direction. The available seismic data have insufficient information on the salt geometries and salt, around-salt, subsalt velocity distribution, but incorporating information from EM has allowed an unambiguous and robust procedure to better constrain the model. For the Espirito Santo study area, we have demonstrated significant imaging improvements that can alter the interpretation.

The results presented in this study were achieved with advanced but available EM and seismic data imaging technologies. The followed workflow is straightforward to integrate into established depth imaging toolboxes. An advantage of this approach is that it utilizes the sensitivities of different data types to different parts of the model. Therefore, we believe that the method can be of use to a wide range of depth imaging groups.

Taking into account for anisotropy, exploiting the complementary information of collocated ultra-long offset seismic and incorporating gravity data into FWI to contribute additional low wavenumbers and independent constraints for the density model, will be key to augment the value of this workflow when applied to wide-aperture

and wide-azimuth seismic and this will be the aim of our future work.

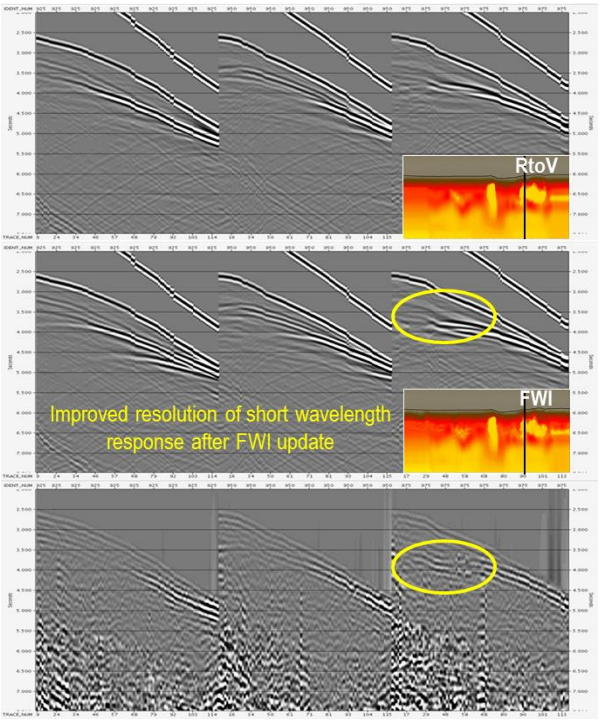

Figure 6: Examples of 7 Hz shot gathers around line QQ CMP 4400: (Upper panel) Computed from broadband CSEM – Resistivity-to-Velocity transform velocity model; (Middle panel) Computed from final FWI velocity model; (Lower panel) from observed seismic.

Acknowledgments

We are thankful to the management of both Petrobras and Schlumberger for support and permission to publish this work. We are extremely grateful for the contribution of Gustavo Basta Dos Santos Silva and Rafael Correia Freitas of Petrobras EXP/IABCS/PN for their great knowledge of the Espirito Santo seismic and geology.

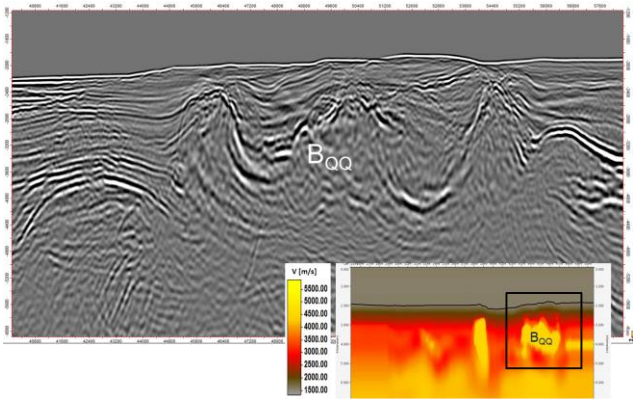

Figure 7: Line QQ – Zoom-in on a detail (salt B_{QQ}) of RTM results using the velocity model from the broadband CSEM – Resistivity-to-Velocity transform workflow (FWI starting model). Significant amount of smearing still present due to lack of details in ToS.

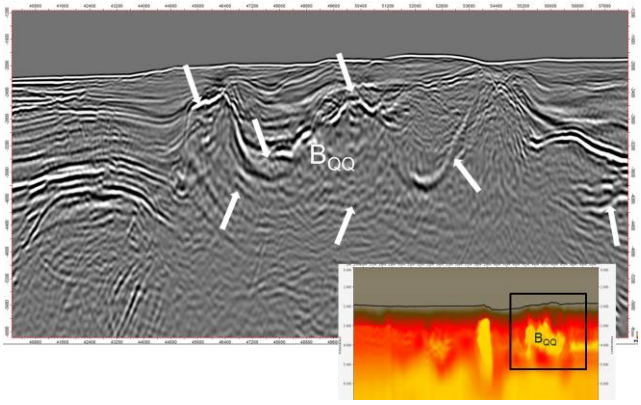

Figure 8: Line QQ – Zoom-in on a detail (salt B_{QQ}) of RTM results using the FWI final velocity model. Image better focused and stacks more powerful. BOS better imaged by reduced amount of reverberations. Smearing footprint of the migration operator reduced by increased model details.

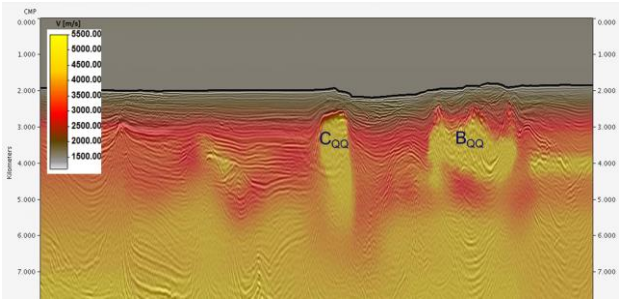

Figure 9: Line QQ – Starting FWI velocity model from the broadband CSEM – Resistivity-to-Velocity transform workflow co-visualized with 20 Hz RTM seismic depth image.

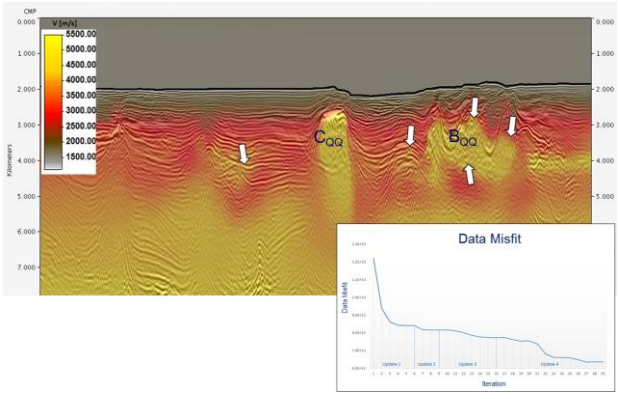

Figure 10: Line QQ – Final FWI velocity model with rms misfit as a function of iterations co-visualized with 20 Hz RTM seismic depth image.

References

De Stefano, M., Andreasi, F.G., Re, S., Virgilio, M., Snyder, F., **2011**, Multiple-domain, simultaneous joint inversion of geophysical data with application to subsalt imaging: Geophysics, 76, 69-80.

Hacikoylu, P., Dvorkin, J., and Mavko, G., **2006**, Resistivity–velocity transforms revisited, Leading Edge, 25, 1006–1009.

Jones, I. F and Davison, I., **2014**, Seismic imaging in and around salt bodies, Special section: Salt basin model building, imaging and interpretation, Interpretation, Vol. 2, No. 4 (November 2014); p. SL1–SL20, 28 FIGS., 1 TABLE.

Medina, E., A. Lovatini, F. G. Andreasi, S. Re, and F. Snyder, **2012**, Simultaneous joint inversion of 3D seismic and magnetotelluric data from the walker ridge: First Break, 30, 85–88.

Moorkamp, M., B. Heincke, M. Jegen, A. Roberts, and R. Hobbs, **2011**, A framework for 3-D joint inversion of MT, gravity and seismic refraction data: Geophysical Journal International, 184, 477–493, doi: 10.1111/j .1365-246X.2010.04856.x.

Panzner, M., W. W. Weibull, and J. P. Morten, **2014**, Sub-basalt imaging in the Faroe-Shetland basin using CSEM&MT data to constrain the velocity model: 84th Annual International Meeting, SEG, Expanded Abstracts, 3806–3810.

Zerilli, A., Labruzzo, T., Buonora, M.P., **2013**, Joint inversion of marine MT and wide aperture seismic data using a 'hybrid'-based approach, Society of Exploration Geophysicist 83rd Annual Meeting and Exposition , 22-27 September, Houston, Texas, 775-779.

Zerilli, A., Labruzzo, T., Zanzi, M., Buonora, M.P., Crepaldi, J.L., Menezes, P.T.L., **2014**, Broadband marine CSEM: New benefits for subsalt and around salt exploration, Society of Exploration Geophysicist 84rd Annual Meeting and Exposition, 26-31 October, Denver, Colorado, 750-754.

Zerilli, A., Miotti, F., Buonora, M.P., Crepaldi, J.L., Menezes, P.T.L., **2016**, Using broadband mCSEM-driven velocity model building to improve complex subsalt imaging, European Association of Geophysical Engineers, 78th Conference & Exhibition, Vienna, Austria, 30 May-2 June.